PHYSICAL REVIEW B **93**, 060403(R) (2016)

Observation of magnon-mediated electric current drag at room temperature

H. Wu,[1] C. H. Wan,[1] X. Zhang,[1] Z. H. Yuan,[1] Q. T. Zhang,[1] J. Y. Qin,[1] H. X. Wei,[1] X. F. Han,[1,*] and S. Zhang[2,†]

[1]*Beijing National Laboratory for Condensed Matter Physics, Institute of Physics, Chinese Academy of Sciences, Beijing 100190, China*

[2]*Department of Physics, University of Arizona, Tucson, Arizona 85721, USA*

(Received 11 October 2015; revised manuscript received 14 January 2016; published 12 February 2016)

Spin-based electronic devices such as magnetic memory and spin logic rely on spin information transport. Conduction electrons, due to their intrinsic spin angular momentum, become an obvious choice for spin information carriers. Here, we experimentally demonstrate that magnons, quasiparticles representing low-energy excitations of ferromagnetic materials, can serve as effective spin information carriers as well. Specifically, we consider two nonmagnetic heavy metals (HMs) that are separated by an electric leak-free ferrimagnetic insulator. When an electric current is applied in one of the HM layers, magnons in the ferrimagnetic insulator are excited and become an effective medium to couple the spin currents in two HMs. As a result, the charge/spin current in one HM layer can drag a charge/spin current in the other HM layer. This work provides a route for spin-based electronic devices where the spin transport is carried by quasiparticles other than electrons.

DOI: 10.1103/PhysRevB.93.060403

The generation, manipulation, and detection of spin current are fundamental issues in spintronics research [1,2]. Spin current represents the flow of spin angular momentum that transfers spin information from one region to another, enabling spin-based information storage and processing [3]. In today's spintronics, conduction electrons play the role of messengers: Giant magnetoresistance (GMR) comes from the electron traveling between two ferromagnetic layers separated by a nonmagnetic layer [4,5], and spin transfer torque (STT) is the result of the electron picking a spin angular momentum from one ferromagnetic layer and releasing it to the other ferromagnetic layer [6–11]. An interesting question is whether other particles or even quasiparticles can serve as spin information carriers.

Magnons are quasiparticles representing a low-energy excited state of ferromagnets. A quantized magnon is a boson and carries basic spin angular momentum quanta of $-\hbar$ [12]. Similar to spintronics and electronics, magnonics refers to using magnons for data storage and information processing [13]. Up to now, magnons in the field of spintronics have been investigated within the content of magnetostatic spin waves which describe the nonuniform spatial and temporal distribution of the classical magnetization vector. The observed spin Seebeck effect in ferrimagnetic insulators has been attributed to such spin wave excitations [14–17]. Recently, a theoretical model has been proposed for observing magnon-mediated electric current drag across a ferrimagnetic insulator layer in a heavy metal (HM)/ ferrimagnetic insulator (FI)/ heavy metal (HM) structure [18,19]. In this theory, an applied electric current in one HM layer accompanies an electron spin current due to the spin Hall effect (SHE) [20–22]. When the spin current flows to the boundary between the HM and the FI, nonequilibrium spins are accumulated and, consequently, due to the *s-d* exchange interaction between conduction electrons in HM and magnetic moments in FI, magnons are created at the interface [23,24]. The induced magnons subsequently diffuse in FI to the other interface where the magnon current converts back to an electron spin current in the other HM layer, leading to a charge current due to the inverse spin Hall effect (ISHE) [25–27]. Thus, the induced electric current in the second HM layer which is electrically insulated from the current-flowing HM layer by a FI would elucidate the magnons as spin information carriers. It is noted that the above magnon-mediated electric current drag is a linear response phenomenon, i.e., the drag current is linearly proportional to the applied current.

There are two important features in the above-described magnon-mediated electric current drag effect. First, the electron-magnon conversion efficiency at the interface increases with temperature since the magnon emission and absorption rates scale with the equilibrium number of magnons. Therefore, the drag effect is larger for higher temperatures. Second, the conversion also depends on the relative orientation between the magnetization of the FI and the applied electric current. For an electric current along the x direction, the spin current would flow in the z direction (perpendicular to the layer) with its spin polarization in the y direction. Angular momentum conservation demands that the induced magnons have their angular momenta in the y direction as well. Therefore, the largest conversion between the electron spin current and the magnon current occurs when magnetization of the FI is orientated in the y direction. Such a magnetization orientation dependence is one of the signatures of the magnon drag effect [18,19].

We note that other related spin transport mechanisms may also transfer electrical signals from one Pt layer to the other through yttrium iron garnet (YIG). In the spin pumping scenario [25,28], the spin current of Pt can be absorbed by YIG, which may generate a precessional motion of YIG [29] and pump a spin current to the other Pt layer, leading to an induced voltage. Another possibility is the spin Seebeck effect, which refers to an induced spin current by a temperature gradient in ferrimagnets [30]. When a current is applied, Joule heating may lead to a small temperature gradient, but the effect will be quadratic with respect to the current. We will discuss the relevance of these two mechanisms after we show our experimental results.

*xfhan@iphy.ac.cn

†zhangshu@email.arizona.edu

 ©2016 American Physical Society

In an early experiment, Kajiwara *et al.* [31] considered an in-plane geometry by depositing two Pt strips, a few millimeters apart, on a YIG surface. When the electric current applied in one Pt bar reaches a critical value, the spin transfer torque [32,33] overcomes the magnetic damping force such that the magnetization of the YIG begins to precess. The precessing YIG then generates spin and charge currents in the second HM layer due to spin pumping. Since a large critical current is required to induce YIG precession, the observed voltage signal is abruptly turned on and then gradually increases with the applied current. Most recently, Cornelissen *et al.* reexamined the above experiment and found a linear relation between the induced voltage and the applied current [34]. This finding indicates that spin transfer torque induced YIG precession might not be the mechanism for their observed effect.

To directly prove that magnon-mediated spin angular momentum flow is responsible for the coupling of the spin currents between two Pt layers, we construct a spin-valve-like trilayer structure where the two Pt layers are sandwiched by a YIG layer. We report below a series of experiments including the structure characterization, and magnetic and spin transport measurements.

Pt(10)/YIG(40,60,80,100)/Pt(10) (thickness in nanometers) as well as reference samples Cu(10)/YIG(60)/Pt(10) and Pt(10)/YIG(60)/Cu(10) were prepared on Si-SiO_2 substrates by an ultrahigh vacuum magnetron sputtering system (ULVAC, MPS-4000). The reference samples were used for accessing possible Joule heating and the resulting spin Seebeck effect. Details of the growth conditions, annealing treatment and patterning, and the methods of magnetic characterization are given in the Supplemental Material [35].

Figure 1(a) shows the schematic illustration of the sample structure. An electric current I_b was applied (Keithley, 2440) along the x axis in the bottom Pt layer, the magnetic field H was applied along the y axis, and the voltage V_t was measured (Keithley, 2182A) along the x axis in the top Pt layer. Figure 1(b) shows the schematic illustration of the spin transport process in the Pt/YIG/Pt structure. The cross-sectional transmission electron microscopy (TEM) and high resolution TEM (HRTEM) of the Pt(10)/YIG(100)/Pt(10) sample were observed by Tecnai G2 F20 S-TWIN (200 kV). There are no pinholes and element diffusion in YIG [see Fig. S1(a) in the Supplemental Material], confirming the insulating properties of YIG. The multilayer is continuous and flat, and each interface (bottom Pt/YIG and top YIG/Pt) is clear and sharp [Fig. 1(c)]. A high quality YIG crystal structure is formed on Pt after high temperature annealing, as shown in Fig. 1(d). The ferromagnetic resonance linewidth of the 60 nm YIG in the Si-SiO_2/Pt(10)/YIG(60)/Pt(10) structure is 358 Oe, which is much larger than that deposited on a $Gd_3Ga_5O_{12}$ (GGG) (111) single crystal (16.4 Oe) [Fig. S1(b)]. This is expected because the crystal quality of the YIG epitaxially grown on the GGG (111) single crystal is usually much better.

Figure 2(a) shows the induced signal V_t/R_t in the top Pt layer as a function of the applied current I_b in the bottom Pt layer, while R_t is the resistance of the top Pt layer. A 1 kOe magnetic field which completely saturates the magnetic moment M of YIG was applied along the y direction. An

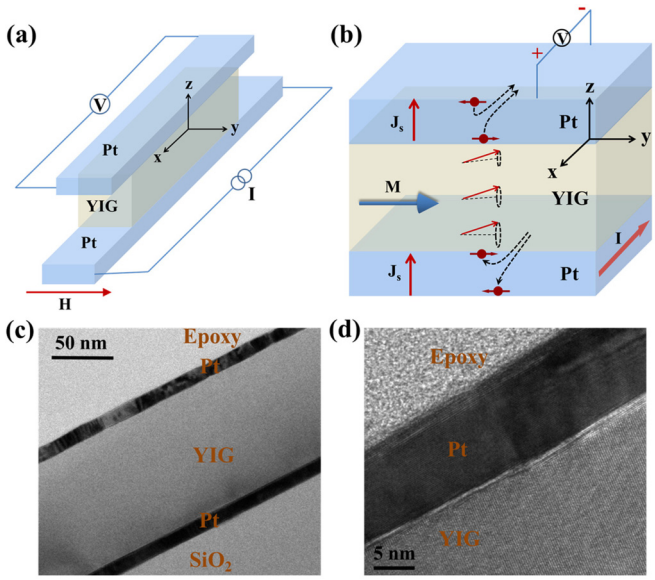

FIG. 1. (a) A schematic illustration of the sample structure and the measurement method. An electric current I_b is applied along the x axis in the bottom Pt layer, the magnetic field H is applied along the y axis, and the voltage V_t is measured along the x axis in the top Pt layer. (b) The proposed spin transport processes in the Pt/YIG/Pt structure. The spin current is generated by the charge current in the bottom Pt layer via the spin Hall effect (SHE), resulting in a spin accumulation at the bottom Pt/YIG interface. Subsequently, the magnon current excited by the spin accumulation diffuses from the bottom to the top interface, and then converts back to the electron spin current in the top Pt layer. Finally, the spin current in the top Pt is detected by the voltage via the inverse spin Hall effect (ISHE). (c) and (d) The cross-sectional transmission electron microscopy (TEM) image of the Pt(10)/YIG(100)/Pt(10) (thickness in nanometers) multilayer and the cross-sectional high resolution TEM (HRTEM) image of the Pt/YIG interface, respectively.

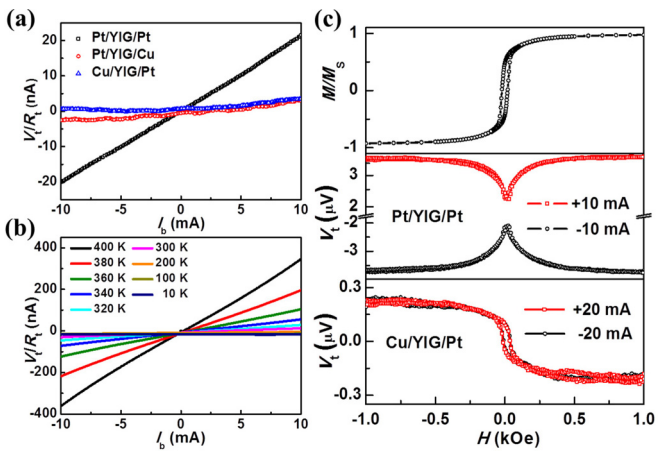

FIG. 2. (a) V_t/R_t-I_b characteristics measured in Pt/YIG/Pt, Cu/YIG/Pt, and Pt/YIG/Cu samples. A 1 kOe magnetic field is applied along the y direction during the measurement. (b) Temperature-dependent V_t/R_t-I_b curves of the Pt/YIG/Pt sample. A 1 kOe magnetic field is applied along the y direction during the measurement. (c) The magnetic field dependence of the magnon drag voltage in Pt/YIG/Pt and the spin Seebeck voltage in Cu/YIG/Pt, which are in accordance with the magnetic properties of YIG as shown in the M-H loop.

approximate linear relation between V_t/R_t and I_b is observed up to a maximum value of $I_b = 8 \times 10^5$ A/cm^2 (10 mA), which is in accord with the magnon drag theory. A small quadratic contribution to the voltage V_t/R_t is possibly a contribution from the spin Seebeck effect, where the Joule heating may induce a temperature gradient across the YIG layer, i.e., $V_t/R_t = aI_b + bI_b^2$, where a is the coefficient of the magnon drag contribution and the small b is from the spin Seebeck effect. The electrical drag coefficient a estimated from Fig. 2(b) is 2.13×10^{-6} at room temperature and 3.41×10^{-5} at 400 K, about two orders of magnitude smaller than the theoretical estimation (10^{-4} at room temperature); this is not surprising since the theoretical estimation was made for perfect interfaces where the spin convertance between the spin current of the electrons and the magnon current is maximized. Magnetic impurity scattering at both the bottom Pt/YIG and top YIG/Pt interfaces can transfer spin angular momenta to the lattice, and thus reduce the spin convertance.

It is interesting to note that the induced voltage signal has the same polarity as the applied current; this can be understood as follows. The spin Hall effect dictates that the directions of the spin current flow $\boldsymbol{J}_s$, the charge current flow $\boldsymbol{J}_e$, and the spin-polarization vector $\boldsymbol{\sigma}$ of spin current are mutually perpendicular, i.e., $\boldsymbol{J}_s = \theta_{SH}\boldsymbol{\sigma} \times \boldsymbol{J}_e$, where θ_{SH} is the spin Hall angle. The induced charge current in the top Pt is $\boldsymbol{J}_e^t \propto \theta_{SH}\boldsymbol{\sigma} \times \boldsymbol{J}_s^t \propto \theta_{SH}\boldsymbol{\sigma} \times \boldsymbol{J}_s^b = \theta_{SH}^2\boldsymbol{\sigma} \times (\boldsymbol{\sigma} \times \boldsymbol{J}_e^b) = -\theta_{SH}^2\boldsymbol{J}_e^b$, where we denote the superscripts t and b as the top and bottom layers and we use the fact that the spin current and magnon current flow in the direction perpendicular to the layer plane throughout the entire trilayer. When one uses a voltmeter to measure the induced voltage in the top Pt layer, one produces a polarity that is the same as the current flow in the bottom Pt layer.

To access the possible contribution from the Joule heating related spin Seebeck effect, we replaced one of the HM layers with Cu, which is known to have a negligibly small spin Hall angle [36]. As expected, V_t/R_t is greatly reduced, indicating no magnon-mediated electric drag. A small value of $V_t/R_t = bI_b^2$ remains present when the Cu is at the bottom, but not at the top. The single Pt layer in contact with YIG would yield a spin Seebeck signal as long as the temperature gradient exists. These results are consistent with the notion that the small induced nonlinear signal in the Cu/YIG/Pt and Pt/YIG/Pt samples is from the spin Seebeck effect. Also, the magnetic field and magnetization direction dependences of the spin Hall magnetoresistance [37,38] in the top and bottom Pt layers of Pt/YIG/Pt were also measured respectively, which confirms the spin conversion between spins in Pt and magnons in YIG (see Figs. S4 and S5 for details).

One of the characteristics in the magnon-mediated electric drag effect is that the electron-magnon conversion efficiency at the interface increases with temperature because the magnon emission and absorption rates scale with the equilibrium number of magnons. For an ideal interface with a simple quadratic magnon dispersion, the drag signal increases with a power of 5/2 of temperature [18,19]. In Fig. 2(b), we show the temperature-dependent magnon drag signal of Pt/YIG/Pt. The electrical drag coefficient a increases sharply with increasing temperature, consistent with the theory. However, the experimental data cannot be fitted by a simple power law. Clearly, a theoretical model, beyond ideal interfaces and a simple magnon dispersion, is needed to thoroughly understand the temperature dependence. We make a further analysis on the data in the Supplemental Material for future theoretical considerations.

The magnetic field dependence of the voltage signal of the Pt/YIG/Pt and Cu/YIG/Pt samples is shown in Fig. 2(c). A 10 mA (20 mA) electric current was applied in the bottom Pt (Cu) layer, and the magnetic field H ($\pm$1 kOe) was scanned along the y axis. For Pt/YIG/Pt samples, the V_t-H curves are symmetric with respect to $\pm H$. The magnon drag voltage is largest when the magnetic moment $\boldsymbol{M}$ of YIG is saturated by the magnetic field along the y axis, and is minimum at the coercive field where the y component of the magnetization is zero. When we reversed the polarity of the electric current in the bottom Pt, the polarity of the measured voltage in the top Pt is also reversed. In contrast, the magnon drag voltage in Cu/YIG/Pt samples is much smaller at any magnetic field. More importantly, the symmetry with respect to the direction of the applied magnetic field and the polarity of the applied current is different: V_t-H curves are asymmetric with $\pm H$, and V_t-H curves are independent of the polarity of the current. These results confirm that the observed voltage signals are dominated by magnon-mediated drag for Pt/YIG/Pt samples, but not for Cu/YIG/Pt samples. Both samples have a small contribution for the spin Seebeck effect.

To establish a definite relation between the magnon drag voltage signal and the direction of the magnetization, we rotate the magnetization direction of YIG in three orthogonal planes by applying a 3 kOe magnetic field which is larger than the saturation field. In magnon drag theory, the electron-magnon current conversion depends on the relative orientation between the magnetization of the FI and the applied electric current. For an electric current along the x direction, the spin current would flow in the z direction (perpendicular to the layer) with its spin polarization in the y direction. Angular momentum conservation demands that the induced magnons have their angular momenta in the y direction as well. Therefore, the voltage signal always scales with the square of the y component of the magnetization, i.e., $V_t \propto m_y^2$. Such a magnetization orientation dependence is one of the signatures of the magnon drag effect [18,19]. We show in Fig. 3 the voltage signal variation as a function of the magnetization angles α, β, and γ. For Pt/YIG/Pt samples, the angular dependence of $V_t \propto m_y^2$ fits excellently with the data [see the dashed lines in Fig. 3(b)], while for Cu/YIG/Pt samples, the much smaller signal comes from the spin Seebeck voltage which could be well fitted by $V_t \propto m_y$, as shown by the dashed lines in Fig. 3(c). The difference in the magnetization direction dependence between the Pt/YIG/Pt and Cu/YIG/Pt samples can clearly distinguish the magnon drag voltage from the spin Seebeck voltage.

Finally, we investigate the decay length of the magnon current in YIG by varying the YIG thickness of the similarly grown Pt/YIG/Pt trilayers from 40 to 100 nm. We attribute the reduction of the signal for the thicker trilayers seen in Fig. 4(a) to a magnon current loss due to magnetic damping in the YIG layer. If we simply fit the thickness dependence by an exponential decay function $a = a_0 e^{-t/l_m}$, we find the magnon decay length l_m is about 38 nm, as shown in Fig. 4(b).

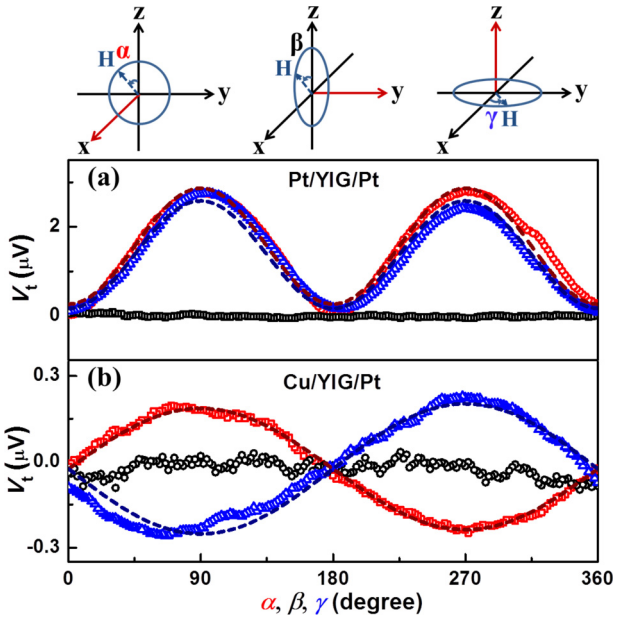

FIG. 3. Top: The definition of the angular α, β, and γ in this figure. A 3 kOe constant magnitude of the magnetic field is applied to saturate the magnetic moment $\boldsymbol{M}$ during the sample rotation. (a) The magnetization direction dependence of the magnon drag voltage in Pt/YIG/Pt. A 10 mA electric current is applied in the bottom Pt layer, and the voltage is measured in the top Pt layer. (b) The magnetization direction dependence of the spin Seebeck voltage in Cu/YIG/Pt. The electric current applied in the bottom Cu is 20 mA, and the voltage is measured in the top Pt layer.

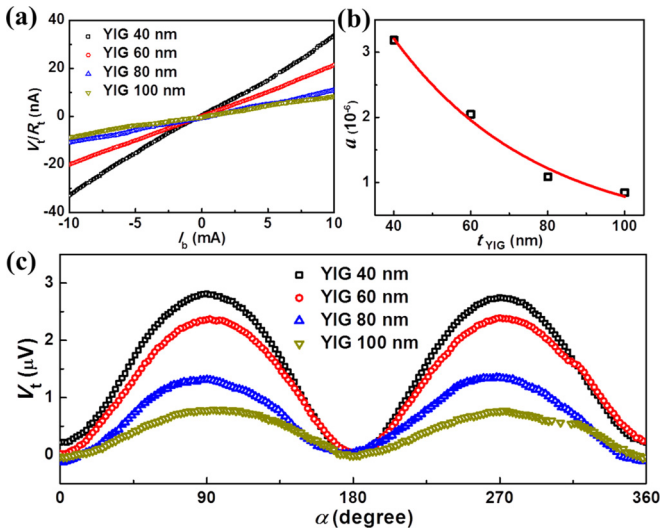

FIG. 4. (a) V_t/R_t-I_b curves of Pt(10)/YIG(t)/Pt(10) samples with different thicknesses (t = 40, 60, 80, 100 nm) of YIG. A 1 kOe magnetic field is applied along the y direction during the measurement. (b) The YIG thickness dependence of the electrical drag coefficient a, while the open squares show the measured data, and the red line shows the fitting curve $a = a_0 e^{-t/l_m}$. (c) The magnetization direction dependence of the magnon drag voltage in Pt/YIG/Pt samples with different thicknesses of YIG. A 10 mA electric current is applied in the bottom Pt layer, and the voltage is measured in the top Pt layer. A 3 kOe constant magnitude of the magnetic field is applied to saturate the magnetic moment $\boldsymbol{M}$ during the sample rotation.

We note that the magnon decay length obtained here is considerably smaller than the conventional one determined from ferromagnetic resonance for single crystalline YIG samples [39]; this discrepancy is expected, considering that our YIG layer is deposited on polycrystalline Pt and thus the spin-dependent scattering from the defects and the grain boundaries are likely much stronger than those in single crystal YIG. A comparable magnon decay length of about 70 nm has been found in YIG/Pt by other groups [40,41]. The magnetization direction dependences for the samples with different thicknesses of YIG are similar, as shown in Fig. 4(c).

In conclusion, we have experimentally observed magnon-mediated electric current drag at room temperature in a Pt/YIG/Pt structure. The dependences of the drag voltage signal on temperature, the polarity of the current, and the direction of magnetization are consistent with the earlier theoretical prediction of magnon current propagation through a ferrimagnetic insulator. Our observed results differ from spin pumping and spin Seebeck induced voltage signals. This work provides a direct and clear observation that quasiparticle magnons can efficiently serve as spin information carriers for spin-based storage and processing applications.

This work was supported by the 863 Plan Project of Ministry of Science and Technology (MOST) (Grant No. 2014AA032904), the MOST National Key Scientific Instrument and Equipment Development Projects (Grant No. 2011YQ120053), the National Natural Science Foundation of China (NSFC) (Grants No. 11434014 and No. 11222432), and the Strategic Priority Research Program (B) of the Chinese Academy of Sciences (CAS) (Grant No. XDB07030200).

[1] S. A. Wolf, D. D. Awschalom, R. A. Buhrman, J. M. Daughton, S. V. Von Molnar, M. L. Roukes, A. Y. Chtchelkanova, and D. M. Treger, Science **294**, 1488 (2001).

[2] I. Žutić, J. Fabian, and S. D. Sarma, Rev. Mod. Phys. **76**, 323 (2004).

[3] D. A. Allwood, G. Xiong, C. C. Faulkner, D. Atkinson, D. Petit, and R. P. Cowburn, Science **309**, 1688 (2005).

[4] M. N. Baibich, J. M. Broto, A. Fert, F. Nguyen Van Dau, F. Petroff, P. Etienne, G. Creuzet, A. Friederich, and J. Chazelas, Phys. Rev. Lett. **61**, 2472 (1988).

[5] G. Binasch, P. Grünberg, F. Saurenbach, and W. Zinn, Phys. Rev. B **39**, 4828 (1989).

[6] B. Özyilmaz, A. D. Kent, D. Monsma, J. Z. Sun, M. J. Rooks, and R. H. Koch, Phys. Rev. Lett. **91**, 067203 (2003).

[7] J. C. Sankey, Y. T. Cui, J. Z. Sun, J. C. Slonczewski, R. A. Buhrman, and D. C. Ralph, Nat. Phys. **4**, 67 (2007).

[8] J. Z. Sun, R. P. Robertazzi, J. Nowak, P. L. Trouilloud, G. Hu, D. W. Abraham, M. C. Gaidis, S. L. Brown, E. J. O'Sullivan, W. J. Gallagher, D. C. Worledge, Phys. Rev. B **84**, 064413 (2011).

[9] L. Liu, C. F. Pai, Y. Li, H. W. Tseng, D. C. Ralph, and R. A. Buhrman, Science **336**, 555 (2012).
[10] A. Brataas, A. D. Kent, and H. Ohno, Nat. Mater. **11**, 372 (2012).
[11] W. J. Jiang, P. Upadhyaya, W. Zhang, G. Q. Yu, M. B. Jungfleisch, F. Y. Fradin, J. E. Pearson, Y. Tserkovnyak, K. L. Wang, O. Heinonen, S. G. E. Velthuis, and A. Hoffmann, Science **349**, 283 (2015).
[12] C. Kittel, *Introduction to Solid State Physics* (Wiley, New York, 2005), Chap.12.
[13] A. V. Chumak, V. I. Vasyuchka, A. A. Serga, and B. Hillebrands, Nat. Phys. **11**, 453, (2015).
[14] K. Uchida, S. Takahashi, K. Harii, J. Ieda, W. Koshibae, K. Ando, S. Maekawa, and E. Saitoh, Nature (London) **455**, 778 (2008).
[15] K. Uchida, J. Xiao, H. Adachi, J. Ohe, S. Takahashi, J. Ieda, T. Ota, Y. Kajiwara, H. Umezawa, H. Kawai, G. E. W. Bauer, S. Maekawa, and E. Saitoh, Nat. Mater. **9**, 894 (2010).
[16] G. E. Bauer, E. Saitoh, and B. J. van Wees, Nat. Mater. **11**, 391 (2012).
[17] H. Wu, C. H. Wan, Z. H. Yuan, X. Zhang, J. Jiang, Q. T. Zhang, Z. C. Wen, and X. F. Han, Phys. Rev. B **92**, 054404 (2015).
[18] S. S.-L. Zhang and S. Zhang, Phys. Rev. Lett. **109**, 096603 (2012).
[19] S. S.-L. Zhang and S. Zhang, Phys. Rev. B **86**, 214424 (2012).
[20] J. E. Hirsch, Phys. Rev. Lett. **83**, 1834 (1999).
[21] Y. K. Kato, R. C. Myers, A. C. Gossard, and D. D. Awschalom, Science **306**, 1910 (2004).
[22] O. Mosendz, J. E. Pearson, F. Y. Fradin, G. E. W. Bauer, S. D. Bader, and A. Hoffmann, Phys. Rev. Lett. **104**, 046601 (2010).
[23] S. Takahashi, E. Saitoh, and S. Maekawa, J. Phys.: Conf. Ser. **200**, 062030 (2010).
[24] S. A. Bender, R. A. Duine, and Y. Tserkovnyak, Phys. Rev. Lett. **108**, 246601 (2012).
[25] E. Saitoh, M. Ueda, H. Miyajima, and G. Tatara, Appl. Phys. Lett. **88**, 182509 (2006).
[26] S. O. Valenzuela and M. Tinkham, Nature (London) **442**, 176 (2006).
[27] T. Kimura, Y. Otani, T. Sato, S. Takahashi, and S. Maekawa, Phys. Rev. Lett. **98**, 156601 (2007).
[28] Y. Tserkovnyak, A. Brataas, and G. E. W. Bauer, Phys. Rev. Lett. **88**, 117601 (2002).
[29] E. Padron-Hernandez, A. Azevedo, and S. M. Rezende, Appl. Phys. Lett. **99**, 192511 (2011).
[30] L. Lu, Y. Sun, M. Jantz, and M. Wu, Phys. Rev. Lett. **108**, 257202 (2012).
[31] Y. Kajiwara, K. Harii, S. Takahashi, J. Ohe, K. Uchida, M. Mizuguchi, H. Umezawa, H. Kawai, K. Ando, K. Takanashi, S. Maekawa, and E. Saitoh, Nature (London) **464**, 262 (2010).
[32] J. C. Slonczewski, J. Magn. Magn. Mater. **159**, L1 (1996).
[33] L. Berger, Phys. Rev. B **54**, 9353 (1996).
[34] L. J. Cornelissen, J. Liu, R. A. Duine, J. Ben Youssef, and B. J. Van Wees, Nat. Phys. **11**, 1022 (2015).
[35] See Supplemental Material at http://link.aps.org/supplemental/10.1103/PhysRevB.93.060403 for sample preparation and measurement method, HAADF result and FMR absorption spectrum, temperature dependence of electrical drag coefficient, magnetic field dependence of magnon drag voltage in x and z directions, SMR in top and bottom Pt, and leakage current test.
[36] H. L. Wang, C. H. Du, Y. Pu, R. Adur, P. C. Hammel, and F. Y. Yang, Phys. Rev. Lett. **112**, 197201 (2014).
[37] S. Y. Huang, X. Fan, D. Qu, Y. P. Chen, W. G. Wang, J. Wu, T. Y. Chen, J. Q. Xiao, and C. L. Chien, Phys. Rev. Lett. **109**, 107204 (2012).
[38] H. Nakayama, M. Althammer, Y. T. Chen, K. Uchida, Y. Kajiwara, D. Kikuchi, T. Ohtani, S. Geprägs, M. Opel, S. Takahashi, R. Gross, G. E. W. Bauer, S. T. B. Goennenwein, and E. Saitoh, Phys. Rev. Lett. **110**, 206601 (2013).
[39] P. Pirro, T. Brächer, A. V. Chumak, B. Lägel, C. Dubs, O. Surzhenko, P. Görnert, B. Leven, and B. Hillebrands, Appl. Phys. Lett. **104**, 012402 (2014).
[40] S. M. Rezende, R. L. Rodríguez-Suárez, R. O. Cunha, A. R. Rodrigues, F. L. A. Machado, G. A. Fonseca Guerra, J. C. Lopez Ortiz, and A. Azevedo, Phys. Rev. B **89**, 014416 (2014).
[41] M. Weiler, M. Althammer, M. Schreier, J. Lotze, M. Pernpeintner, S. Meyer, H. Huebl, R. Gross, A. Kamra, J. Xiao, Y. T. Chen, H. J. Jiao, Gerrit E. W. Bauer, and Sebastian T. B. Goennenwein, Phys. Rev. Lett. **111**, 176601 (2013).